Biosensors and Bioelectronics 26 (2011) 2858–2863

Contents lists available at ScienceDirect

Biosensors and Bioelectronics

journal homepage: www.elsevier.com/locate/bios

Fabrication of a carbon fiber paper as the electrode and its application toward developing a sensitive unmediated amperometric biosensor

Chiun-Jye Yuan[a,b,*], Chung-Liang Wang[a], Teng Yang Wu[a], Kuo-Chu Hwang[c], Wei-Chi Chao[a]

[a] Department of Biological Science and Technology, National Chiao Tung University, Hsinchu, Taiwan, ROC
[b] Institute of Molecular Medicine and Bioengineering, National Chiao Tung University, Hsinchu, Taiwan, ROC
[c] Department of Chemistry, National Tsing Hua University, Hsinchu, Taiwan, ROC

ARTICLE INFO

Article history:
Received 27 August 2010
Received in revised form
15 November 2010
Accepted 16 November 2010
Available online 24 November 2010

Key words:
Amperometric biosensor
Carbon fiber paper
Nitrogen plasma
Phenolic compounds
Tyrosinase

ABSTRACT

Carbon fiber paper (CFP), a material frequently used as the diffusion layer in fuel cells, was found recently to exhibit a potential as an electrode for the development of sensitive, unmediated biosensors. After nitrogen plasma treatment, the CFP exhibited a quasi-reversible behavior to the redox couple (e.g., ferricyanide) with an electron transfer rate constant of 7.2×10^{-3} cm s^{-1}. This rate constant is approximately double that of a Pt-electrode and is much higher than that of many carbon-based electrodes. The unmediated CFP-based tyrosinase biosensor fabricated for this study exhibited an optimal working potential and operating pH value of −0.2 V and 6.5, respectively. Compared to other unmediated tyrosinase biosensors, the CFP-based tyrosinase biosensor offers a high sensitivity for the monitoring of phenolic compounds (17.8, 7.1, 5.2 and 3.7 μA μM^{-1} cm^{-2} for catechol, phenol, bisphenol and 3-aminophenol, respectively). The lowest detection limit for catechol, phenol, bisphenol and 3-aminophenol was 2, 5, 5 and 12 nM, respectively. Furthermore, this biosensor exhibited a good repeatability, a fast response time (around 10 s), and a wide linear dynamic range of detection for phenolic compounds.

1. Introduction

Carbon fiber paper (CFP) is an electrically conducting carbon paper that is formed by laminating the randomly arranged short carbon fibers in a two-dimensional sheet (Mathur et al., 2007). CFP has been widely used as the diffusion layer in chemical fuel cells (Gharibi and Mirzaie, 2003; Reshetenko et al., 2007; Song et al., 2006) and biofuel cells (Kamitaka et al., 2007; Kuwahara et al., 2008; Tamaki et al., 2007) due to its high-mechanical strength, conductivity and excellent gas permeability. In addition, CFP exhibits several properties, such as low electrical resistivity, easy handling, and high electrochemical stability that make it an ideal electrode material for the development of biosensors.

A tyrosinase-based amperometric biosensor was fabricated in this study for the detection of phenolic pollutants to investigate into the feasibility of the use of CFP in the design and development of biosensors. Phenolic compounds are one of the major organic wastes found in wastewater from industries of manufacturing paints, pesticides, polymeric resin, chemicals and dyes, and from industries of coal conversion and petroleum refinery (Ahmaruzzaman, 2008; Kaisheva et al., 1996; Svitel and Miertus, 1998). Many of these phenolic compounds have been demonstrated to have a harmful effect on animals and plants due to their easy absorption through skin and membranes, their persistence in the environment and their potent genotoxic, mutagenic and hepatotoxic effects (Jaafar et al., 2006; Ahmaruzzaman, 2008; Notsu and Tatsuma, 2004; Reddy et al., 1989; Saha et al., 1999; Yager et al., 1990). They also affect biocatalytic reaction rates in respiration in animals and the photosynthesis of plants. Therefore, many phenolic compounds are listed as dangerous substances, and many countries have enacted environmental legislation to restrict the pollution caused by these compounds (Vincent, 1991). Therefore, it is of great importance to develop a quick, sensitive and easily operated biosensing system to aid the detection of phenolic compound contamination in environmental, industrial and food samples.

Many methods have been developed for the measurement of phenolic compounds, such as colorimetry, gas chromatography, liquid chromatography, capillary electrophoresis and spectrophotometric analysis (Hou et al., 2003; Poerschmann et al., 1997; Wang et al., 2000). However, these methods typically require tedious procedures for sample preparation and the skills of well-trained technician to make them working functionally and efficiently. This limits the application of these methods in routine on-site screening of pollutants. For these reasons, the electrochemical detection of phenolic compounds has received much attention because of its

* Corresponding author at: Department of Biological Science and Technology, National Chiao Tung University, 75 Po-Ai Street, Hsinchu 300, Taiwan, ROC. Tel.: +886 3 5731735; fax: +886 3 5729288.
E-mail address: cjyuan@mail.nctu.edu.tw (C.-J. Yuan).

0956-5663/$ – see front matter © 2010 Elsevier B.V. All rights reserved.
doi:10.1016/j.bios.2010.11.023

simplicity, high sensitivity and quick detection to phenols (Li et al., 2005; Lindgren et al., 1997; Tembe et al., 2008; Zhang et al., 2009).

In this study, the electrochemical properties of CFP were investigated. The surface properties as well as the electrochemical responses of the CFP were shown to be greatly improved by simple nitrogen plasma treatment. CFP-based amperometric biosensors used to detect phenolic compounds, such as phenol, catechol, bisphenol A (BPA) and 3-aminophenol (3AP), were also fabricated by immobilizing tyrosinase on the CFP surface. The tyrosinase is an enzyme that catalyzes hydroxylation and oxidation of mono and diphenols to *o*-quinones, and the electrochemical reduction of these quinones was employed to monitor this reaction (Supplemental Scheme 1). Screen-printed carbon paste (SPCE) electrodes have been widely used in commercial and portable biosensor designs due to its low cost and suitability for mass production. However, low electrochemical responses to many analytes and a low rate of electron transfer are the major disadvantages of SPCE. Hence, the performance of tyrosinase-based phenolic compound biosensors fabricated on CFP and SPCE was also investigated and compared. The results showed that the tyrosinase-based biosensor fabricated on CFP exhibited a higher sensitivity to phenolic compounds and a wide dynamic range of detection than biosensors fabricated on SPCE.

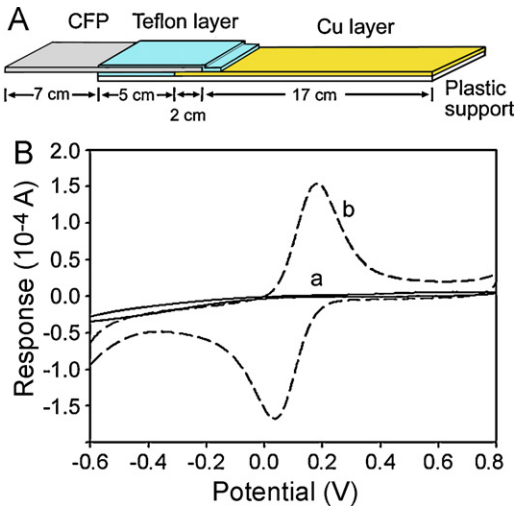

Fig. 1. Fabrication and characterization of CFP electrode. (A) Schematic showing the fabrication of a CFP-based electrode. (B) The cyclic voltammograms of 700 μM ferricyanide on the CFP (curve a) and the CFP^{P} (curve b) electrodes were determined in a reaction chamber containing PBS, pH 6.5 within a potential between −0.6 V and 0.8 V vs. Ag/AgCl. The scan rate was 120 mV s^{-1}.

2. Materials and methods

2.1. Reagents

CFP TGP-H-060 (thickness: 0.17 cm) was purchased from Toray Ind. (Japan). Teflon glue was supplied by DuPont (USA). Tyrosinase (EC 1.14.18.1, 5370 U/mg from mushroom) and catechol (99%) were bought from Sigma–Aldrich. Poly vinyl alcohol functionalized with pyridinium methyl sulfate (PVA-SbQ) was bought from Toyo Gosei Kogyo Co. Ltd. (Japan). SPCE was bought from ApexBichem (Hsinchu, Taiwan). BPA (98%) and 3AP (98%) were purchased from Fluka. Phenol (90%) was purchased from Riedel-de Haën. All other reagents were reagent grade.

2.2. Apparatus

A potentiostat CHI 440 (CH Instruments, West Lafayette, IN, USA) connected to a personal computer was used for the measurement of electrochemical responses of biosensors to phenolic compounds. The three-electrode electrochemical system contained a working electrode (CFP), a counter electrode (a platinized electrode) and a reference electrode (Ag/AgCl). The three electrodes were immersed in a reaction chamber containing 10 mL phosphate buffer saline (PBS) (137 mM NaCl, 2.7 mM KCl, 10 mM Na_2HPO_4, 1.76 mM KH_2PO_4, pH 6.8). The solution in the reaction chamber was stirred at a fixed rate during the reaction.

2.3. Nitrogen plasma treatment

The CFP was pre-treated with nitrogen (N_2) plasma at atmospheric pressure. The treatment was performed with N_2 plasma that jetted out of a nozzle directly onto the surface of the CFP. The nozzle was situated 1 cm above the surface of CFP. The power of the plasma was set between 253 V and 260 V with a current of 2.3 A. The scan rate was set at 5 cm s^{-1} with a scan length of 0.3 cm.

2.4. Preparation of the enzyme electrode

The working electrode was prepared as presented in Fig. 1A. Briefly, a supporting plastic strip (0.3 cm × 2.4 cm) was first covered by a piece of copper foil adhesive tape (0.3 cm × 1.9 cm) to form a conducting surface. The remaining area (0.3 cm × 0.5 cm) was then covered with Teflon glue to form an insulating layer. CFP (0.3 cm × 1.4 cm) was then partially bound on the supporting strip (0.7 cm in length) at the side covered with Teflon film, allowing a 0.2 cm wide area of CFP to directly contact with copper foil. The remaining part of the CFP (0.7 cm in length) overhung from the supporting strip and acted as a working electrode. The surface of CFP outside the working area (0.3 cm × 0.7 cm) was insulated with the Teflon film to prevent unwanted redox reactions.

PVA-SbQ/tyrosinase mixture was first prepared by mixing 16% PVA-SbQ stock solution with tyrosinase stock solution (50 Units μL^{-1} in pH 6.8 PBS buffer) in a 1:1 ratio (v/v). PVA-SbQ/tyrosinase mixture (2.5 μL) was spread on the surface of the plasma-pre-treated CFP electrode or SPCE (with a working area of 0.2 cm × 0.65 cm). SPCEs were pre-treated with cyclic voltammetry in a PBS buffer (pH 7.4) between 0 and 2 V for 10 cycles prior to enzyme immobilization. The PVA-SbQ/tyrosinase/CFP or PVA-SbQ/tyrosinase/SPCE electrode was then sealed in a box containing saturated glutaraldehyde vapor at 4 °C for 12 h to allow cross-linking reactions to occur. Photo-polymerization of PVA-SbQ was achieved by placing the enzyme electrode on ice under an illuminating light for 2 h. The enzyme electrodes were then washed once with PBS buffer (pH 6.5) prior to storage in PBS buffer at 4 °C over night before use.

2.5. Water droplet test

Water droplet tests were performed by observing the contact angle (θ) of a water droplet (10 μL) on the surface of CFP with and without plasma treatment. The contact angle (θ) was determined by measuring the angle between the tangential line of a hemispherical droplet at the surface contacting point and a line parallel to the surface (Wang et al., 2009; Yuan et al., 2009).

2.6. X-ray photoelectron spectroscopy and scanning electron microscope

The CFP electrode (0.2 cm × 0.2 cm) was sputter coated with platinum (12 V, 90 s) before being examined by a thermal field emission scanning electron microscope (JEOL, JSM-6500). X-ray photoelectron spectroscopy (XPS) was performed using the Thermo VG Scientific Theta Probe in the College of Engineering of

National Taiwan University of Science and Technology. Briefly, CFP was cut into a size of 1 cm × 1 cm and dried at 37 °C over night prior to the X-ray scan. The surface of CFP was scanned ten times with a beam size of 15–400 μm (X-ray gun diameter) and an electron jet power of 2.0–100 W at a working pressure of 2.5×10^{-9} Torr. The value from the last scan was recorded and analyzed.

2.7. Experimental procedure

A pH profile study was performed in 100 mM phosphate buffer with pH values between 4.5 and 8.5. Working cyclic voltammetry and amperometric measurements of the developed biosensors were carried out in PBS buffer at a pH of 6.5. The working potential was maintained at −0.2 V vs. Ag/AgCl for amperometric experiments.

3. Results and discussion

3.1. Characterization of the CFP electrode

Scanning electron microscopy showed that CFP is composed of micrometer-scale graphite fibers that form a network-like structure with a large surface area (Supplemental Fig. S1A). The surface hydrophilicity of CFP was then studied by measuring the contact angle (θ) of a water droplet on its surface (Yuan et al., 2009). Supplemental Fig. S1B (top panel) shows that the water droplet on the CFP was round in shape with a contact angle of around 90°. This demonstrated that the surface of the CFP was hydrophobic and may block the access of aqueous electroactive substances to the surface of the electrode. In previous work, we demonstrated that the surface properties of a carbon-based electrode could be greatly improved by plasma treatment (Wang et al., 2009). CFP was therefore treated with nitrogen plasma at room temperature for about 0.24 s. The effect of plasma treatment was apparent due to the marked reduction in contact angle of the water droplet ($\theta = 28°$) on nitrogen plasma-treated CFP (CFP^P) (Supplemental Fig. S1B, bottom panel).

Interestingly, plasma treatment resulted in a marked improvement in the electrochemical properties of the CFP electrode, as demonstrated by cyclic voltammetric study. No distinguishable redox peaks were observed in the cyclic voltammograms (CV) of ferricyanide on CFP (Fig. 1B, curve a). In comparison, the CV of ferricyanide was greatly improved on CFP^P (Fig. 1B, curve b) with the oxidative (E_{pa}) and reductive peak potentials (E_{pc}) and peak-to-peak potential separation (ΔE_p) of 175 mV, 58 mV and 117 mV, respectively. Moreover, the ratio of peak currents (I_{ox}/I_{re}) for ferricyanide approached 1 on CFP^P. These results suggest that the nitrogen plasma treatment leads to a quasi-reversible electrochemical behavior of ferricyanide/ferrocyanide redox couple (Eq. (1)) on the CFP^P electrode:

$$[Fe(CN)_6]^{-4} \underset{\text{Red}}{\overset{\text{Ox}}{\rightleftarrows}} [Fe(CN)_6]^{-3} + 1e^- \quad (1)$$

The chemical composition of elements and their chemical state on the surface of CFP and CFP^P were further analyzed by XPS, a quantitative surface analysis technique. The majority of the elements on the surface of CFP were found to be carbon (284.3 eV) (99 at.% or mean atomic percentage). Other elements, such as oxygen (532.20 eV) and nitrogen (399.50 eV), were only present at concentrations of 0.34 at.% each. However, after nitrogen plasma treatment, the content of oxygen and nitrogen on CFP^P dramatically increased by 29-fold (9.8 at.%) and 9-fold (3.22 at.%), respectively, while the relative content of carbon decreased to 87 at.%. The functional groups present on the surface of CFP were calculated from curve fitting of the C1s narrow spectrum. Two predominant chemical bonds, C=C (284.38–284.53 eV) and C–C (285.11–285.5 eV)

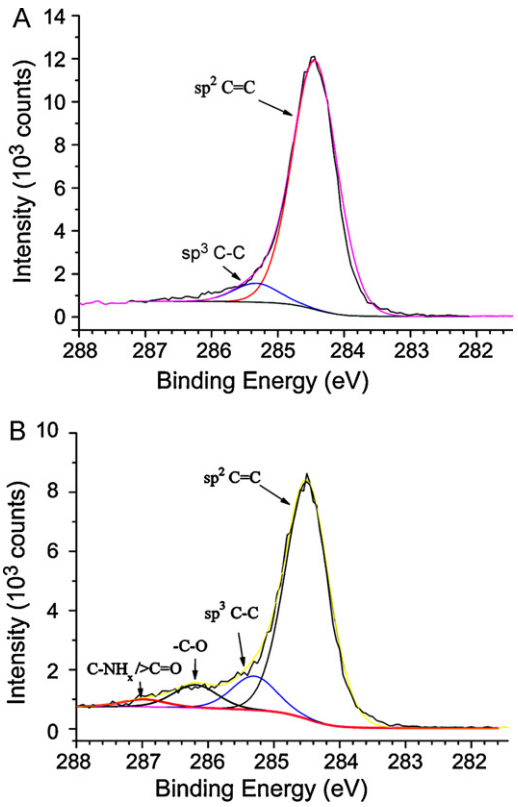

Fig. 2. Surface functional groups analysis of CFP by XPS. The surface functional groups of untreated (A) and plasma-treated CFP (B) were estimated by XPS through curve fitting of the C1s peak area.

(Wang et al., 2009), were detected on CFP (Fig. 2A). However, on the surface of CFP^P, other functional groups, such as –C–O (286.3 eV), >C=O (286.45–287.92 eV) and C–NH_x (286–288.5 eV) (Wang et al., 2009), were found in addition to C=C and C–C (Fig. 2B). These results indicated that various oxygen- and nitrogen-containing functional groups are formed on the surface of CFP after nitrogen plasma treatment. The significant improvement of electrochemical properties and surface hydrophilicity of CFP^P after plasma treatment is likely due to the formation of these functional groups (Tenent and Wipf, 2009; Wang et al., 2009).

3.2. Cyclic voltammetric studies of plasma-treated CFP electrode

Cyclic voltammograms of CFP^P to 1 mM ferricyanide at different scan rates were carried out to determine the electrochemical properties and electron transfer rate constant of CFP after plasma treatment (Fig. 3A). The plots of anodic (I_{pa}) and cathodic (I_{pc}) peak currents were linearly increasing with the scan rate ($\nu^{1/2}$) increased from 20 to 140 mV s^{-1} (Fig. 3A, inset). The corresponding linear regression equations were found to be I_{pa} (μA) = $16.26\nu^{1/2} + 3.156$ ($R = 0.9965$) and I_{pc} (μA) = $-14.93\nu^{1/2} - 2.137$ ($R = 0.9947$). The peak-to-peak separation also increased with the increase of scan rate. These results suggest that a diffusion-controlled process may occur on the surface of CFP^P electrode.

A small peak-to-peak separation (ΔE_p) between redox peaks indicated a fast electron transfer rate. The electron transfer rate constant (k_s) was estimated using the equation $\Psi = k^0[\pi Dn\nu F/(RT)]^{-1/2}$ (Lavagnini et al., 2004; Nicholson, 1965), where k^0 is the heterogeneous electron transfer rate constant of an uncomplicated quasi-reversible electrochemical reaction, n the electron transfer number, ν (V s^{-1}) the scan rate, F the Faraday constant, and R and T the gas constant and absolute temperature (298 K), respectively. The diffusion coefficient (D) used

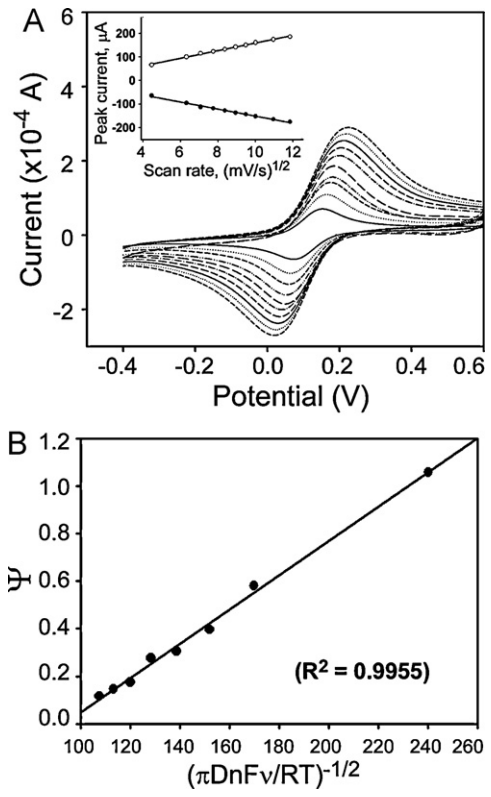

Fig. 3. Cyclic voltammograms of ferricyanide on CFP^P electrode. (A) Cyclic voltammograms of 1 mM ferricyanide on CFP^P were carried out in PBS (pH 6.5) at a potential between −0.4 V and 0.6 V and with scan rates of 20, 40, 60, 80, 100, 120, 140, 160, 180 and 200 mV s^{-1}. (Inset) Plot of anodic (open circle) and cathodic (close circle) peak currents vs. square root of scan rate ($\nu^{1/2}$) for CFP^P electrode. (B) Plot of Ψ vs. $[\pi Dn\nu F/(RT)]^{-1/2}$ was for the estimation of electron transfer rate constant on CFP^P electrode.

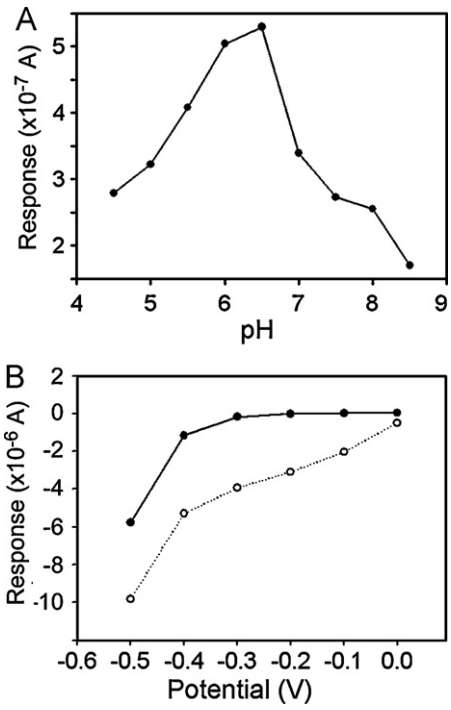

Fig. 4. Optimization of tyrosinase-CFP^P biosensor. (A) The pH-dependence of the Tyrosinase-CFP^P biosensor was investigated in 100 mM phosphagte buffers with different pH value (4.5, 5, 5.5, 6, 6.5, 7, 7.5, 8 and 8.5). The responses to catechol (0.1 μM) under the working potential of −0.2 V vs. Ag/AgCl was recorded and analyzed. (B) The optimal working potential for tyrosinase-CFP^P biosensor was studied by using catechol as a model. Constant reductive currents were measured in PBS (pH 6.5) without (close circle) or with 1 μM catechol (open circle) with constant stirring under potentials ranging from 0.0 to −0.5 V. Each data point is the mean ± S.D. from three independent measurements.

was 7.09×10^{-6} cm^2 s^{-1}(Durgbanshi and Kok, 1998). Ψ was estimated under different scan rates using the empirical equation: $\Psi = (-0.6288 + 0.0021X)/(1 - 0.017X)$, where, X is ΔE_p expressed in mV (Lavagnini et al., 2004). The k^0 was then calculated from the slope of a plot of Ψ vs. $[\pi DnF/(RT)]^{-1/2}\nu^{-1/2}$ (Fig. 3B) to be 7.2×10^{-3} cm s^{-1}. This value is about twice as fast as that of the Pt electrode ($k^0 = \sim 4.0 \times 10^{-3}$ cm s^{-1}) (Taylor and Humffray, 1973), and much faster than that of the carbon paste electrode ($k^0 = 3.6 \times 10^{-4}$ cm s^{-1}) (Lavagnini et al., 2004), un-oxidized GCE ($k^0 = 1.2 \times 10^{-5}$ to 9.2×10^{-5} cm s^{-1}) (Tenent and Wipf, 2009) and oxidized GCE ($k^0 = 9.0 \times 10^{-4}$ cm s^{-1}) (Taylor and Humffray, 1973).

3.3. Fabrication and characterization of the enzyme electrode

The feasibility of using CFP^P in the fabrication of a biosensor was investigated. A tyrosinase-based biosensor (tyrosinase-CFP^P) was fabricated by immobilizing tyrosinase (36 U) on the CFP^P electrode using 8% PVA-SbQ. PVA-SbQ was chosen because it was shown previously to stabilize the immobilized enzyme for at least 3 months (Chang et al., 2003; Lee et al., 2007). In this study the tyrosinase-CFP^P biosensor was shown to retain most of its activity at 4 °C for at least one week (data not shown). The electrochemical response of catechol on the tyrosinase-CFP^P electrode was first investigated by CV. Catechol (200 μM) exhibited clear redox peaks on the tyrosinase-CFP^P electrode with the anodic and cathodic peak potentials of +0.28 V and −0.019 V, respectively (Supplemental Fig. S2A). In comparison, the CV of 200 μM catechol on a SPCE-based tyrosinase biosensor (tyrosinase-SPCE) had the anodic and cathodic peak potentials of +0.39 V and −0.27 V, respectively (Supplemental Fig. S2B). This suggests that CFP exhibits better electrochemical properties than that of SPCE.

The pH dependence of the enzyme electrode was studied by its amperometric response to 0.1 μM catechol in 100 mM phosphate buffers at different pH values (from 4.5 to 8.5). Fig. 4A shows that the optimum response current was achieved in the pH range 6.0–6.5. In order to achieve maximum sensitivity, a pH of 6.5 was maintained in subsequent experiments. The optimal working potential for the detection of phenolic compounds on CFP- and SPCE-based biosensors was investigated. The net steady state redox responses of 1 μM catechol on tyrosinase-CFP^P under potentials between 0 and −0.5 V were recorded and compared with the responses of untreated electrode (Fig. 4B, open circle). The background current of tyrosinase-CFP^P was low over the potential range tested (0.0 V to −0.3 V) (Fig. 4B, close circle). A rapid increase in the magnitude of background current started at −0.4 V. In comparison, the net reductive currents of tyrosinase-CFP^P to 1 μM catechol at potentials of −0.1, −0.2 and −0.3 V were 2.3, 3.1 and 3.9 μA, respectively (Fig. 4B, open circle). Although the electrochemical response of tyrosinase-CFP^P to catechol was higher at −0.3 V, a working potential of −0.2 V vs. Ag/AgCl may be suited for the measurement of phenolic compounds. The use of this working potential may avoid interference from electroactive impurities in samples.

3.4. Responses of the enzyme electrode to phenolic compounds

Fig. 5A shows typical current–time plots of the tyrosinase-CFP^P biosensor at room temperature with successive additions of 100 nM of 3AP, BPA, phenol or catechol to the PBS (pH 6.5). The experiments

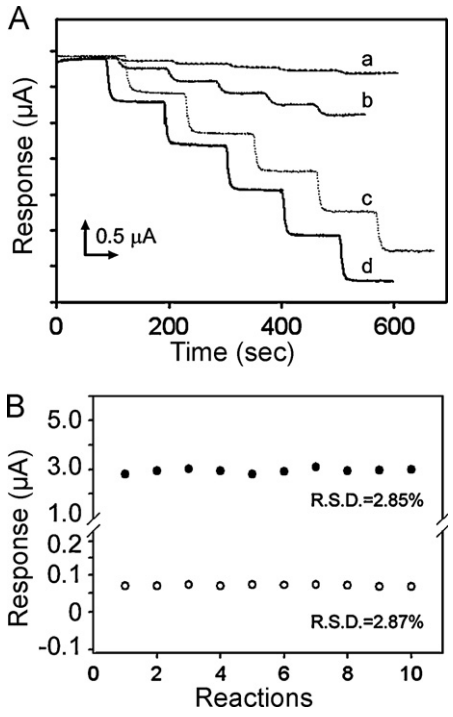

Fig. 5. Characterization of tyrosinase-CFP^P biosensor. (A) Amperometric response of the tyrosinase-CFP^P biosensor to successive additions of 100 nM of 3AP (a), BPA (b), phenol (c) and catechol (d) was determined in PBS (pH 6.5) with constant stirring. (B) Repeatability of the tyrosinase-CFP^P biosensor. Repetitive measurements of the responses of tyrosinase-CFP^P electrode to 1 μM catechol (close circle) and 50 nM BPA (open circle) were carried out 10 times in PBS (pH 6.5) with constant stirring. The working potential was set at −0.2 V vs. Ag/AgCl.

were continued until an equilibrium state was reached. A steady-state baseline current was reached quickly as the tyrosinase-CFP^P biosensor responded rapidly to the incremental addition of phenol, catechol, BPA and 3AP with a response time (95% of the steady-state current) of 10 s, 10 s, 20 s and 18 s, respectively. The biosensor also exhibited a good repeatability of 2.87% and 2.85% relative standard deviation (R.S.D.) for a repetitive measurements of 50 nmol L^{-1} BPA (n = 10) and 1 μM catechol (n = 10), respectively (Fig. 5B). The result shows that the fabricated tyrosinase-CFP^P biosensor exhibits good operational stability and stable sensitivity to BPA and catechol in multiple-usage and continuous analysis.

3.5. Calibration plots of tyrosinase-CFP biosensor to phenolic compounds

The linear dynamic range of detection for various selected phenolic compounds was also determined. The linear dynamic range and correlation coefficient of catechol, phenol, BPA and 3AP on the tyrosinase-CFP^P biosensor were 1.0×10^{-8} to 1.5×10^{-5} M (R^2 = 0.997), 1.0×10^{-8} to 1.5×10^{-5} M (R^2 = 0.996), 1.0×10^{-8} to 1.0×10^{-6} M (R^2 = 0.998) and 2.0×10^{-8} to 1.0×10^{-6} M (R^2 = 0.999), respectively (Supplemental Fig. S3). The sensitivity of the developed biosensor was 17.8, 7.1, 5.2 and 3.7 μA μM^{-1} cm^{-2} for catechol, phenol, BPA and 3AP, respectively (Supplemental Fig. S3). In comparison, the sensitivity of the tyrosinase-SPCE biosensor to catechol and phenol was 1.38 and 1.1 μA μM^{-1} cm^{-2}, respectively (Supplemental Fig. S4 and Table 1). The lowest limit of detection (LOD) (S/N ≥ 3) for catechol, phenol, BPA and 3AP on the tyrosinase-CFP^P biosensor was 2, 5, 5 and 12 nM, respectively. In comparison, the linear dynamic range for catechol and phenol detection on the tyrosinase-SPCE biosensor was 4.0×10^{-8} M to 2.0×10^{-5} M (r^2 = 0.999) and 4.0×10^{-8} M to 1.0×10^{-5} M (r^2 = 0.998), respectively, with a lowest detection limit of 20 nM and 20 nM, respectively.

3.6. Comparison of the performance of the proposed biosensor to existing designs

The performance of the tyrosinase-CFP^P biosensor was compared with those of unmediated-biosensors that have been developed previously (Table 1). It can be seen that the tyrosinase-CFP^P biosensor exhibited a similar linear range of detection for the indicated phenolic compounds compared to the previously developed unmediated-biosensors (Table 1). However, the sensitivity of tyrosinase-CFP^P biosensor to phenol (1490 μA mM^{-1}) and catechol (3740 μA mM^{-1}) is significantly greater than those of GCE-based (Li et al., 2006; Shengfu et al., 2008; Vedrine et al., 2003; Zhang et al., 2003) and carbon paste electrode-based tyrosinase biosensors (Andreescu and Sadik, 2004; Serra et al., 2002). Additionally,

Table 1
Comparison of the performance of various unmediated tyrosinase-based biosensors for phenolic compounds.

Compound	Immobilization method/electrode	Linear range (μM)	Sensitivity (μA mM^{-1})	Detection limit (nM)	Response time (s)
Catechol	PVA-SbQ/CFP[a]	0.01–15	3740	2	10
	PVA-SbQ/SPCE[a]	0.04–20	179	20	25
	Nano-Fe_3O_4-chitosan/GCE[b]	0.083–70	514	25	2
	Nano-ZnO-chitosan/GCE[c]	0.1–75	114	30	10
	Graphite–EPD terpolymer[d]	0.09–8	660	28	–
	Conducting polymer/GCE[e]	?–25	140[f]	–	20–40
	Tyr-CPE[g]	1–20	208.5	25	120
Phenol	PVA-SbQ/CFP[a]	0.01–15	1490	5	10
	PVA-SbQ/SPCE[a]	0.04–10	144	20	25
	Nano-Fe_3O_4-chitosan/GCE[b]	0.083–83	228	25	2
	Nano-ZnO-chitosan/GCE[c]	0.15–65	182	50	10
	Graphite–EPD terpolymer[d]	0.05–6	620	26.3	–
	Conducting polymer/GCE[e]	?–25	42.6[f]	50	20–40
	Hybride titania sol–gel matrix/GCE[h]	0.075–6	1605	10	10

[a] This study.
[b] Shengfu et al. (2008).
[c] Li et al. (2006).
[d] Serra et al. (2002).
[e] Vedrine et al. (2003).
[f] Recalculated from original result 1999 mA M^{-1} cm^{-2} for catechol and 608 mA M^{-1} cm^{-2} for phenol (Vedrine et al., 2003).
[g] Andreescu and Sadik (2004).
[h] Zhang et al. (2003).

the tyrosinase-CFP^{P} biosensor exhibited a lower detection limit for phenol (5 nM) and catechol (2 nM) and a faster response time of 10 s (Table 1). These results suggest that the use of CFP as an electrode has great potential in the fabrication of biosensors for various purposes. Although CFP was shown to exhibit a great potential as an electrode for the development of biosensors, fragile and high cost are drawbacks that may restrict its application in the development of commercial biosensors. More studies are probably needed to facilitate the future application of CFP in the fabrication of biosensors.

4. Conclusion

CFP, a material commonly used in the fabrication of fuel cells, was found in this study to exhibit great potential in the fabrication of biosensors. However, untreated CFP is very hydrophobic and exhibits a relatively low response to electroactive agents. Once treated with nitrogen plasma, CFP becomes hydrophilic and has greatly improved its electrochemical properties, such as a high rate of electron transfer and the existence of quasi-reversible processes. A CFP-based tyrosinase biosensor was fabricated to explore its potential in the development of an amperometric biosensor. Interestingly, the CFP-based tyrosinase biosensor exhibited a high sensitivity to phenolic compounds, such as catechol, phenol, BPA and 3AP, with the lowest detection limit ($S/N \geq 3$) of 2, 5, 5 and 12 nM, respectively. Furthermore, it featured a linear dynamic range of detection to phenolic compounds relative to that of existing tyrosinase biosensors (Andreescu and Sadik, 2004; Li et al., 2006; Serra et al., 2002; Shengfu et al., 2008; Vedrine et al., 2003; Zhang et al., 2003) and had a short response time of 10–20 s. The CFP-based tyrosinase biosensor in this study also exhibited a good repeatability (R.S.D.) of around 2.87%.

Acknowledgement

This work was financially supported by the ATU plan of the Ministry of Education and National Science Council, Taiwan, ROC under contract No. NSC-97-2311-B-009-001 MY3.

Appendix A. Supplementary data

Supplementary data associated with this article can be found, in the online version, at doi:10.1016/j.bios.2010.11.023.

References

Ahmaruzzaman, M., 2008. Adv. Colloid Interface Sci. 143, 48–67.
Andreescu, S., Sadik, O.A., 2004. Anal. Chem. 76, 552–560.
Chang, K.-S., Hsu, W.-L., Chen, H.-Y., Chang, C.-K., Chen, C.-Y., 2003. Anal. Chim. Acta 481, 199–208.
Durgbanshi, A., Kok, W.T., 1998. J. Chromatogr. A 798, 289–296.
Gharibi, H., Mirzaie, R.A., 2003. J. Power Sources 115, 194–202.
Hou, L., Shen, G., Lee, H., 2003. J. Chromatogr. A 985, 107–116.
Jaafar, A., Musa, A., Lee, Y.H., Nadarajah, K., Hamidah, S., 2006. Sens. Actuators B 114, 604–609.
Kaisheva, A., Iliev, I., Kazareva, R., Christov, S., Wollenberger, U., Scheller, F., 1996. Sens. Actuators B 33, 39–43.
Kamitaka, Y., Tsujimura, S., Setoyama, N., Kajino, T., Kano, K., 2007. Phys. Chem. Chem. Phys. 9, 1793–1801.
Kuwahara, T., Ohta, H., Kondo, M., Shimomura, M., 2008. Bioelectrochemistry 74, 66–72.
Lavagnini, I., Antiochia, R., Magno, F., 2004. Electroanalysis 16, 505–506.
Lee, C.-H., Wang, S.-C., Yuan, C.-J., Wen, M.-F., Chang, K.-S., 2007. Biosens. Bioelectron. 22, 877–884.
Li, N., Xue, M.-H., Yao, H., Zhu, J.-J., 2005. Anal. Bioanal. Chem. 383, 1127–1132.
Li, Y.F., Liu, Z.M., Liu, Y.L., Yang, Y.H., Shen, G.L., Yu, R.Q., 2006. Anal. Biochem. 349, 33–40.
Lindgren, A., Emnéus, J., Ruzgas, T., Gorton, L., Marko-Varga, G., 1997. Anal. Chim. Acta 347, 51–62.
Mathur, R.B., Maheshwari, P.H., Dhami, T.L., Tandon, R.P., 2007. Electrochim. Acta 52, 4809–4817.
Nicholson, R.S., 1965. Anal. Chem. 37, 1351–1355.
Notsu, H., Tatsuma, T., 2004. J. Electroanal. Chem. 566, 379–384.
Poerschmann, J., Zhang, Z.Y., Kopinke, F.D., Pawliszyn, J., 1997. Anal. Chem. 69, 597–600.
Reddy, M.V., Blackburn, G.R., Schreiner, C.A., Mehlman, M.A., Makerer, C.R., 1989. Environ. Health Perspect. 82, 253–257.
Reshetenko, T.V., Kim, H.T., Krewer, U., Kweon, H.J., 2007. Fuel Cells 7, 238–245.
Saha, N.C., Bhunia, F., Kaviraj, A., 1999. Bull. Environ. Contam. Toxicol. 63, 195–202.
Serra, B., Jiménez, S., Mena, M.L., Reviejo, A.J., Pingarrón, J.M., 2002. Biosens. Bioelectron. 17, 217–226.
Shengfu, W., Yumei, T., Dongming, Z., Guodong, L., 2008. Biosens. Bioelectron. 23, 1781–1787.
Song, J.M., Suzuki, S., Uchida, H., Watanabe, M., 2006. Langmuir 22, 6422–6428.
Svitel, J., Miertus, S., 1998. Environ. Sci. Technol. 32, 828–832.
Tamaki, T., Ito, T., Yamaguchi, T., 2007. J. Phys. Chem. B 111, 10312–10319.
Taylor, R.J., Humffray, A.A., 1973. J. Electroanal. Chem. 42, 347–354.
Tembe, S., Chaudhari, P.S., Bhoraskar, S.V., D'Souza, S.F., Karve, M.S., 2008. Sens. J. IEEE 8, 1593–1597.
Tenent, R.C., Wipf, D.O., 2009. J. Solid State Electrochem. 13, 583–590.
Vedrine, C., Fabriano, S., Tran-Minh, C., 2003. Talanta 59, 535–544.
Vincent, G., 1991. In: Angeletti, G., Bjorseth, A. (Eds.), Organic Micropollutants in the Aquatic Environment. Kluwer Academic Publisher, Dordrecht, NL, pp. 285–292.
Wang, H., Li, J., Liu, X., Yang, T., Zhang, H., 2000. Anal. Biochem. 281, 15–20.
Wang, S.C., Chang, K.S., Yuan, C.J., 2009. Electrochim. Acta 54, 4937–4943.
Yager, J.W., Eastmond, D.A., Robertson, M.L., Paradisin, W.M., Smith, M.T., 1990. Cancer Res. 50, 393–399.
Yuan, C.-J., Wang, Y.-C., Reiko, O., 2009. Anal. Chim. Acta 653, 71–76.
Zhang, J., Lei, J., Liu, Y., Zhao, J., Ju, H., 2009. Biosens. Bioelectron. 24, 1858–1863.
Zhang, T., Tian, B., Kong, J., Yang, P., Liu, B., 2003. Anal. Chim. Acta 489, 199–206.